MAGNETOHYDRODYNAMICS Vol. 51 (2015), No. 2, pp. 321–327

VALIDITY OF QUASI-2D MODELS FOR MAGNETO-CONVECTION

L. Bühler[1], *C. Mistrangelo*[1], *S. Molokov*[2]

[1] *Karlsruhe Institute of Technology (KIT), Postfach 3640, 76021 Karlsruhe, Germany*
e-Mail: leo.buehler@kit.edu
[2] *Coventry University, Priory Street, Coventry CV1 5FB, UK*

For applications in nuclear fusion reactors where magnetic fields are very strong, liquid metal flows in the cores of ducts can often be regarded as inertialess and practically inviscid, while viscous effects are localized in thin boundary layers. The intense electromagnetic Lorentz forces, resulting from the interaction of induced electric currents and imposed magnetic field, tend to remove flow variations along magnetic field lines and they force the fluid to circulate mainly in planes perpendicular to the field. The established quasi-two dimensional magnetohydrodynamic flow can be predicted by means of an approximate model by reducing the basic governing equations to a 2D problem by analytical integration along magnetic field lines. Such models have been applied in the past by numerous authors to investigate duct flow problems and magneto-convection. However, limitations of those Q2D approaches have never been systematically studied.

Introduction. Liquid metal flows in strong magnetic fields are dominated by Lorentz forces, while viscous effects are confined to very thin boundary layers. The flow in the inviscid cores is highly correlated along magnetic field lines and changes of variables in this direction are often negligible. This fact has been exploited in the past to derive quasi-two dimensional (Q2D) model equations following the ideas proposed by Sommeria and Moreau (1982) [1]. Q2D models enable an efficient solution of 3D MHD problems, e.g., for shear flow instabilities [2] [3], DNS simulations of Q2D turbulent flows [4], including heat transfer and buoyant flows [5, 6, 7], interpretation of experimental data [8, 9], or simulations for fusion blanket applications [10]. It has been shown that results for inertial isothermal flows obtained by the Q2D model can be further improved by a proper modelling of inertia terms, which leads to “barrel” or “cigar” shape flow patterns aligned along the magnetic field [11, 12] instead of pure 2D structures.

The purpose of the present work is showing that Q2D models may have significant deficits for particular classes of buoyant flows, a fact that is not at all obvious from a first point of view. As an example, we consider buoyant MHD flows in a horizontal liquid metal layer of height H, length lH and width $2aH$, Fig. 1.

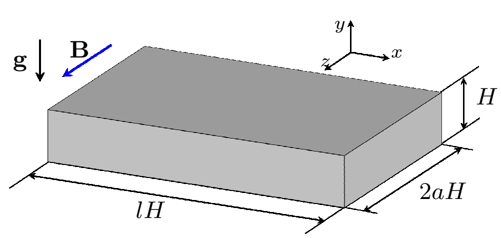

Fig. 1. Sketch of geometry and coordinates. The flat cavity, filled with liquid metal, is differentially heated at $x/H = \pm 1/2$, such that a mean axial temperature gradient $G\hat{\mathbf{x}}$ establishes. Top and bottom walls at $y/H = \pm 1/2$ have temperature profiles that vary linearly between the values of the differentially heated walls. The other walls are adiabatic. The convective motion is damped by a horizontal magnetic field in the z-direction.

We apply the Q2D model equations and compare results with 3D numerical simulations of full governing equations. Such geometries are typical in horizontal Bridgman crystal growth or for liquid metal blankets of fusion reactors.

1. Model equations. Buoyant flows of incompressible, viscous, electrically conducting fluids in a uniform horizontal magnetic field are described by nondimensional equations for a balance of energy, momentum and mass, by the Ohms law and by an electric potential equation to ensure charge conservation $\nabla \cdot \mathbf{j} = 0$:

$$\mathrm{Pr}\,\mathrm{D}_t T = \nabla^2 T, \tag{1}$$

$$\mathrm{D}_t \mathbf{u} + \nabla p - \nabla^2 \mathbf{u} = \mathrm{Gr} T \hat{\mathbf{y}} + \mathrm{Ha}^2 (\mathbf{j} \times \mathbf{B}), \tag{2}$$

$$\nabla \cdot \mathbf{u} = 0, \tag{3}$$

$$\mathbf{j} = -\nabla \phi + \mathbf{u} \times \mathbf{B}, \tag{4}$$

$$\nabla^2 \phi = \nabla \cdot (\mathbf{u} \times \mathbf{B}) = \mathbf{B} \cdot \boldsymbol{\omega}. \tag{5}$$

Here T, $\mathbf{u}$, $\mathbf{B} = B\hat{\mathbf{z}}$, $\mathbf{j}$, p and ϕ stand for the temperature difference with respect to a reference value, velocity, magnetic field, current density, pressure and electric potential scaled by characteristic values ΔT, u_0, B_0, $\sigma u_0 B_0$, $\sigma u_0 B_0^2 H$ and $u_0 B_0 H$, respectively.

Dimensionless parameters are the Prandtl number, the Grashof number and the Hartmann number:

$$\mathrm{Pr} = \frac{\nu}{\kappa}, \quad \mathrm{Gr} = \frac{g\beta H^3 \Delta T}{\nu^2}, \quad \mathrm{Ha} = B_0 H \sqrt{\frac{\sigma}{\rho\nu}}. \tag{6}$$

Kinematic viscosity ν, thermal diffusivity κ and electrical conductivity σ are assumed to be constant, ρ is the density at the reference temperature and β is the coefficient of volumetric thermal expansion. B_0 is a typical magnitude of the magnetic field, $u_0 = \nu/H$ is a characteristic velocity and ΔT is derived from the mean horizontal temperature gradient $G\hat{\mathbf{x}}$ as $\Delta T = GH$. At all walls we have no-slip $\mathbf{u} = 0$. If walls are electrically conducting, currents may continue their path inside the walls and create there a distribution of the wall potential ϕ_w according to the thin-wall condition [13], $\mathbf{j} \cdot \mathbf{n} = c\nabla_\mathrm{w}^2 \phi_\mathrm{w}$, where $c = \sigma_\mathrm{w} t_\mathrm{w}/(\sigma H)$ is the conductance parameter of walls with conductivity σ_w and thickness t_w, ∇_w is the gradient in the plane of the wall and the unit normal $\mathbf{n}$ points into the fluid.

It is well known that for strong magnetic fields, $Ha \gg 1$, the flow takes place preferentially in planes perpendicular to $\mathbf{B}$, i.e. $\mathbf{u} \approx \mathbf{u}_\varepsilon$, and it is described by an equation for the field-aligned component ω_z of vorticity $\boldsymbol{\omega} = \nabla \times \mathbf{u}_\perp$ that is obtained by taking the curl of Eq. (2)

$$(\nabla \times \mathrm{D}_t \mathbf{u}_\perp)_z - \nabla^2 \omega_z = \mathrm{Gr}\,\partial_x T + \mathrm{Ha}^2 \partial_z j_z. \tag{7}$$

Following the ideas usually referred to as the Q2D approach (see [1] and others), the vorticity equation (7) and the potential equation (5) are integrated along magnetic field lines (the overbar above variables denotes average along field lines):

$$\left(\overline{\nabla \times \mathrm{D}_t \mathbf{u}_\perp}\right)_z - \nabla_\perp^2 \overline{\omega}_z - \frac{1}{a}\partial_z \omega_z (z = a) = \mathrm{Gr}\,\partial_x \overline{T} + \mathrm{Ha}^2 \frac{1}{a} j_z (z = a), \tag{8}$$

$$\nabla_\perp^2 \overline{\phi} + \frac{1}{a}\partial_z \phi_z (z = a) = \nabla_\perp^2 \overline{\phi} - \frac{1}{a} j_z (z = a) = \overline{\omega}_z. \tag{9}$$

When Q2D models are applied, it is usually assumed that the potential does not change along magnetic field lines, $\overline{\phi} = \phi(z = a) = \phi_H$. With the thin-wall condition $j_z(z = a) = -c\nabla_\perp^2 \phi_H$ [13] and viscous friction $\partial_z \omega_z(z = a) = -\mathrm{Ha}\,\overline{\omega}_z$ applied at the Hartmann wall, j_z and $\overline{\phi} = \phi_H$ can be eliminated from Eqs. (8) and (9) and the Q2D equation for vorticity becomes

$$\left(\overline{\nabla \times \mathrm{D}_t \mathbf{u}_\perp}\right)_z - \nabla_\perp^2 \overline{\omega}_z = \mathrm{Gr}\,\partial_x \overline{T} - \underbrace{\left(\frac{c\mathrm{Ha}^2}{a+c} + \frac{\mathrm{Ha}}{a}\right)}_{1/\tau} \overline{\omega}_z. \tag{10}$$

Instead of solving Eq. (10), we may solve the following model equation, the curl of which yields Eq. (10):

$$\overline{\mathrm{D}_t \mathbf{u}_\perp} - \nabla_\perp^2 \overline{\mathbf{u}}_\perp + \nabla_\perp \overline{p} = \mathrm{Gr}\overline{T}\hat{\mathbf{y}} - \frac{1}{\tau}\overline{\mathbf{u}}_\perp \quad \text{with} \quad \nabla \cdot \overline{\mathbf{u}}_\perp = 0. \tag{11}$$

The model derived above is valid only for a *uniform* horizontal temperature gradient, as shown in the following. For liquid metals with $\mathrm{Pr} \ll 1$ conduction of heat governs Eq. (1) which supports the ansatz $T = x + \mathrm{Pr}\,\theta$, where θ describes deviations from pure heat conduction. Flows with $\mathrm{Gr} \gg 1$ and $\mathrm{Ha} \gg 1$ are dominated by the right-hand side of Eq. (7) through a balance between Lorentz forces and buoyancy, and for $\mathrm{Pr} \ll 1$ the current density and potential become approximately

$$-\partial_z j_z = \partial_{zz}\phi = \frac{\mathrm{Gr}}{\mathrm{Ha}^2}\partial_x T \approx \frac{\mathrm{Gr}}{\mathrm{Ha}^2}. \tag{12}$$

By integration along z, the potential ϕ and its mean value $\overline{\phi}$ along z are determined as

$$\phi = \phi_H + \frac{\mathrm{Gr}}{2\mathrm{Ha}^2}\left(z^2 - a^2\right) \quad \text{and} \quad \overline{\phi} = \phi_H - \frac{a^2\mathrm{Gr}}{3\mathrm{Ha}^2}, \tag{13}$$

where the potential ϕ_H at the Hartmann wall at $z = a$ has been introduced as an integration function. Already at leading order the potential ϕ is not at all uniform in the core along the field lines. For flows, where $\partial_x \overline{T} \neq \text{const}$, the last term in Eq. (13) depends also on (x, y) and, finally, an additional contribution will appear in Eq. (11). Moreover, the electric properties of field-aligned walls never enter into the Q2D model, although their conductance may have an essential impact on the global closure of current paths with severe consequences for the flow structure. This will be shown in the following by some selected examples.

2. Results.

2.1. Insulating walls. Let us first consider flows in cavities with walls that are electrically poorly conducting or insulating, as considered for instance in [7]. Results from numerical simulations using the Q2D model and full 3D equations are compared (the latter ones with up to $8.6 \cdot 10^6$ grid points, all layers well resolved, grid-independent results achieved).

Contours of the velocity magnitude for $a = 1$, $\mathrm{Pr} = 0.015$, $\mathrm{Gr} = 10^7$, $\mathrm{Ha} = 1000$, $c = 0$ are shown in Fig. 2. It can be observed that a single stationary global recirculation establishes. Near the hot and cold ends of the geometry the fluid moves upward and downward, respectively, while in the central part the flow is preferentially horizontal and aligned parallel to the mean temperature gradient. A qualitative comparison displayed in the figure shows already good agreement between Q2D and 3D simulations. This is further confirmed by comparing the velocity and the temperature along a vertical line in the middle of the cavity, as shown in Fig. 3. For parameters used in the simulation, the Q2D model is able to predict well the velocity distribution in the core and reasonably well the decay towards the field aligned walls at $y = \pm 1/2$. Nevertheless, one can observe still

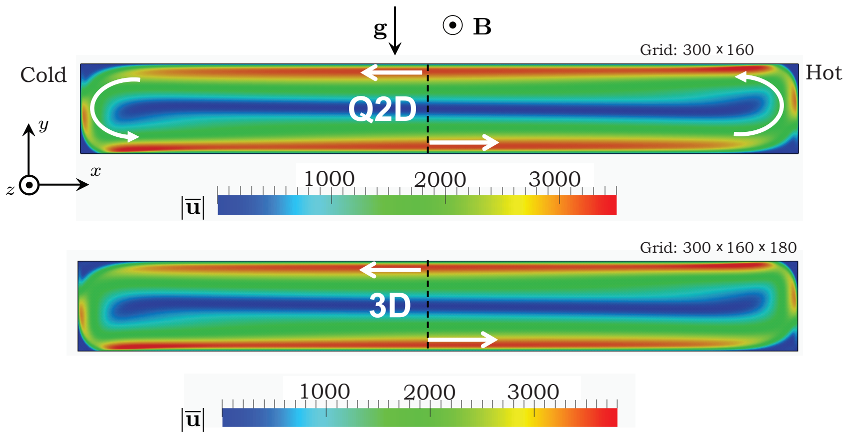

Fig. 2. Colored contours of the velocity magnitude in the vertical symmetry plane $z = 0$ obtained by Q2D and 3D simulations for $a = 1$, $\mathrm{Gr} = 10^7$, $\mathrm{Pr} = 0.015$, $\mathrm{Ha} = 1000$, $c = 0$.

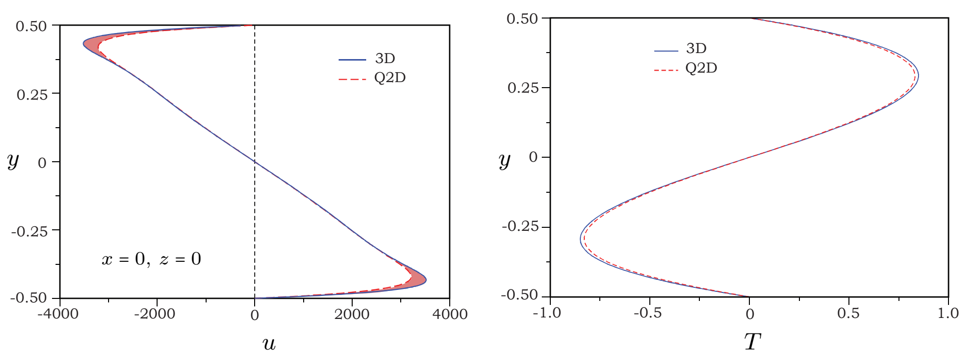

Fig. 3. Comparison of axial velocity and temperature along y at $(x, z) = (0, 0)$ obtained by Q2D and 3D simulations for $a = 1$, $\mathrm{Gr} = 10^7$, $\mathrm{Pr} = 0.015$, $\mathrm{Ha} = 1000$, $c = 0$.

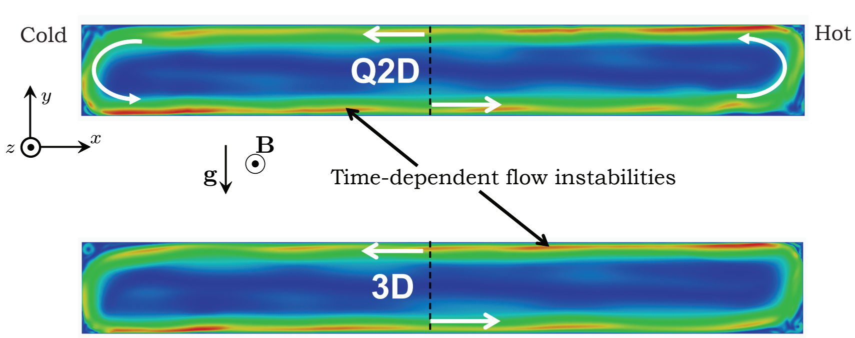

Fig. 4. Colored contours of the velocity magnitude in the vertical symmetry plane $z = 0$ obtained by Q2D and 3D simulations for $a = 1$, $\mathrm{Gr} = 10^8$, $\mathrm{Pr} = 0.015$, $\mathrm{Ha} = 1000$, $c = 0$.

minor differences between the Q2D model and 3D simulations. More precisely, the Q2D model slightly underestimates the velocity when approaching top and bottom walls. The prediction of the vertical temperature distribution is also good.

When the Grashof number is increased to Gr = 10^8, the flow intensifies and the initially laminar stationary motion becomes unstable and shows time-dependent undulated flow patterns along the horizontal walls. This behavior is also well predicted by the Q2D model in accordance with 3D simulations, as shown in Fig. 4. However, as expected (see Fig. 3), the velocity predicted by the Q2D model is a bit smaller than the one from 3D simulations.

2.2. Conducting walls. As a second case, we consider magneto-convection in a perfectly electrically conducting cavity with $c = \infty$. Fig. 5 shows contours of the velocity magnitude in the vertical symmetry plane $z = 0$ for $a = 1$, Gr = 10^8, Pr = 0.015, Ha = 1000. We observe already a strong qualitative disagreement between Q2D and 3D simulations. While Q2D solutions show a more or less smooth velocity field, 3D simulations predict a low velocity core and thin boundary layers with a very high velocity along walls at $y = \pm 1/2$ and $x = \pm l/2$. Results deviate by more than one order of magnitude. This can be seen by a quantitative comparison of axial velocity profiles, as shown in Fig. 6. However, the significant disagreement is present only in layers along parallel walls, while in the core the two solutions agree quite well. Nevertheless, since the layers carry the major mass flux, a 3D simulation is mandatory and Q2D results are practically useless, as can be seen also by a comparison of the temperature profiles in the middle of the cavity (Fig. 6). The flow rate in field aligned layers that is missing in the Q2D model can

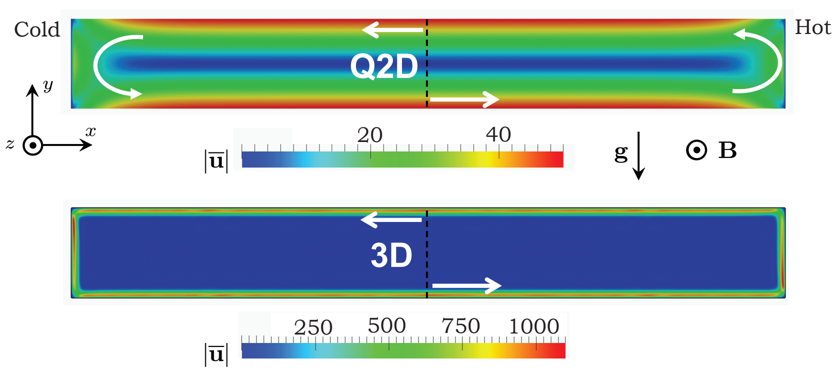

Fig. 5. Colored contours of the velocity magnitude in the vertical symmetry plane $z = 0$ obtained by Q2D and 3D simulations for $a = 1$, Gr = 10^8, Pr = 0.015, Ha = 1000, $c = \infty$.

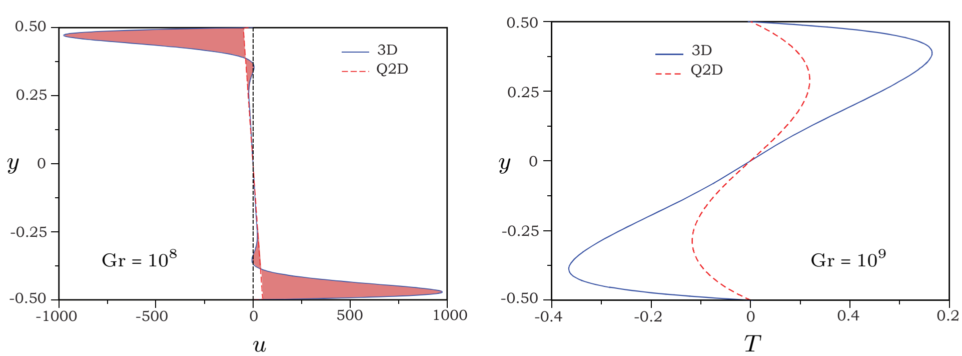

Fig. 6. Comparison of axial velocity and temperature along y at $(x, z) = (0, 0)$ obtained by Q2D and 3D simulations for $a = 1$, Pr = 0.015, Ha = 1000, $c = \infty$.

be estimated according to [14], e.g., at the upper wall for a cross-section $x = \text{const}$ as

$$Q_\delta = \int_{-a}^{a}\int_{\delta} u \mathrm{d}y\mathrm{d}z = -\int_{-a}^{a}\int_{\delta} \partial_y \phi \mathrm{d}y\mathrm{d}z = -2a\int_{\delta} \partial_y \overline{\phi} \mathrm{d}y = -2a\left(\overline{\phi}_{\mathrm{w}} - \overline{\phi}_\delta\right) = -2a\frac{a^2\mathrm{Gr}}{3\mathrm{Ha}^2}. \quad (14)$$

Here $\int_\delta \mathrm{d}y$ indicates integration across the layer. For perfectly conducting walls $\phi_{\mathrm{w}} = 0$, while the potential $\overline{\phi}_\delta$ at the edge of the layer is given by Eq. (13). The vorticity in the core at leading order may be estimated from Eq. (10) as $\overline{\omega}_z = \partial_x \overline{v} - \partial_y \overline{u} = \tau\mathrm{Gr}$, from which the axial core flow rate in the upper half of the cavity results by integration as

$$Q_{\mathrm{c}} = \int_{-a}^{a}\int_{0}^{1/2} u \mathrm{d}y\mathrm{d}z = -\frac{a}{4}\frac{\mathrm{Gr}}{\mathrm{Ha}^2}. \quad (15)$$

This simple estimate shows clearly that the error in the not-considering parallel layers in Q2D models can be significant. Further 3D simulations with perfectly conducting Hartmann walls and insulating field-aligned walls show an additional increase in side layer velocity by another order of magnitude compared to the previous case with $c = \infty$, so that a comparison with corresponding Q2D results becomes even worse.

3. Conclusions. Q2D models had been often applied in the past as efficient tools for numerical simulations of various MHD phenomena for $\mathrm{Ha} \gg 1$. In the present work, it has been shown that those models may have severe deficits, for instance, since the electrical conductivity of field-aligned walls is not considered. Moreover, for the derivation of Q2D models it is usually assumed that the electric potential is uniform along magnetic field lines, an assumption that is not justified for convection problems. A comparison with 3D numerical simulations suggests that for electrically insulating walls Q2D models give reasonable estimates for velocity and heat transfer for both stationary and time-dependent flows. For electrically conducting walls, however, Q2D results become useless so that 3D simulations are mandatory.

Acknowledgements. This project has received funding from the European Union's Horizon 2020 research and innovation program under grant agreement no. 633053. The views and opinions expressed herein do not necessarily reflect those of the European Commission.

REFERENCES

[1] J. Sommeria and R. Moreau. Why, how, and when MHD turbulence becomes two-dimensional. *J. Fluid Mechanics*, vol. 118 (1982), pp. 507–518.

[2] L. Bühler. Instabilities in quasi-two-dimensional magnetohydrodynamic flows. *J. Fluid Mechanics*, vol. 326 (1996), pp. 125–150.

[3] N. Vetcha, S. Smolentsev and M. Abdou. Linear stability analysis for the Hartmann flow with interfacial slip. *Magnetohydrodynamics*, vol. 48 (2012), no. 1, pp. 147–155.

[4] S. Smolentsev and R. Moreau. Modeling quasi-two-dimensional turbulence in MHD duct flows. *Proc. the Summer Program 2006* (CTR, Stanford University, 2006), pp. 419–430.

[5] W.K. Hussam and G.J. Sheard. Heat transfer in a high Hartmann number MHD duct flow with a circular cylinder placed near the heated side-wall. *International Journal of Heat and Mass Transfer*, vol. 67 (2013), pp. 944–954.

[6] S. Smolentsev, N. Vetcha and M. Abdou. Effect of a magnetic field on stability and transitions in liquid breeder flows in a blanket. *Fusion Engineering and Design*, vol. 88 (2013), no. 6–8, pp. 607–610.

[7] A.Y. Gelfgat and S. Molokov. Quasi-two-dimensional convection in a three-dimensional laterally heated box in a strong magnetic field normal to main circulation. *Physics of Fluids*, vol. 23 (2011), no. 3, pp. 034101-1–13.

[8] L. Barleon, P. Jochmann, K.J. Mack, U. Burr and R. Stieglitz. Experimental investigations on the magneto-convective flow in a vertical gap. *Proc. the 4th International Conference on Energy Transfer in Magnetohydrodynamic Flows* (Giens, France, 2000).

[9] U. Burr and U. Müller. Rayleigh-Bénard convection in liquid metal layers under the influence of a horizontal magnetic field. *J. Fluid Mechanics*, vol. 453 (2002), pp. 345–369.

[10] E. Mas de les Valls, L. Batet, V. de Medina, J. Fradera, M. Sanmartí and L. Sedano. Influence of thermal performance on design parameters of a He/LiPb dual coolant DEMO concept blanket design. *Fusion Engineering and Design*, vol. 87 (2012), pp. 969–973.

[11] A. Pothérat, J. Sommeria and R. Moreau. An effective two-dimensional model for MHD flows with transverse magnetic field. *J. Fluid Mechanics*, vol. 424 (2000), pp. 75–100.

[12] B. Mück, C. Günther, U. Müller and L. Bühler. Three-dimensional MHD flows in rectangular ducts with internal obstacles. *J. Fluid Mechanics*, vol. 418 (2000), pp. 265–295.

[13] J.S. Walker. Magnetohydrodynamic flows in rectangular ducts with thin conducting walls. *Journal de Mécanique*, vol. 20 (1981), no. 1, pp. 79–112.

[14] M.S. Tillack and K. McCarthy. *Flow quantity in side layers for MHD flow in conducting rectangular ducts* (Techn. Rep. UCLA-IFNT-89-01, 1989).

Received 07.01.2015